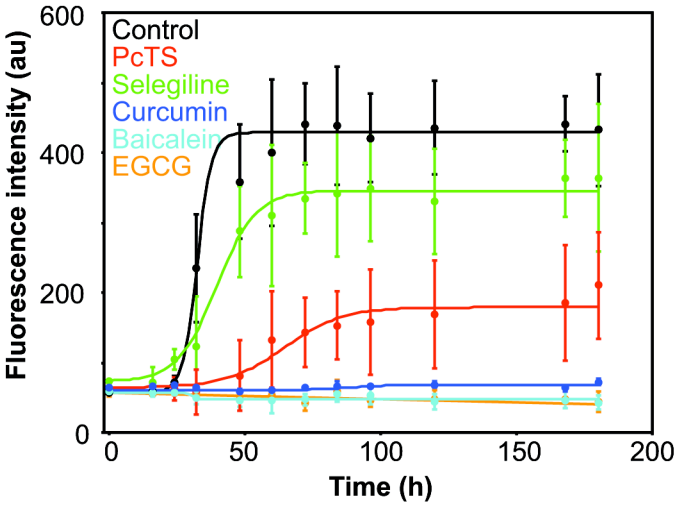

Supplementary Figure 1 | Influence of selected small molecules on fibril formation of disordered αSyn in solution. Fibril formation kinetics in aggregation prone conditions (37 °C with stirring). The concentration of αSyn was 100 μM. 15-fold excess of compound over protein was used. The final DMSO concentration was 1% of the total volume. Error bars represent ± standard deviation from the mean of at least 3 different experiments.

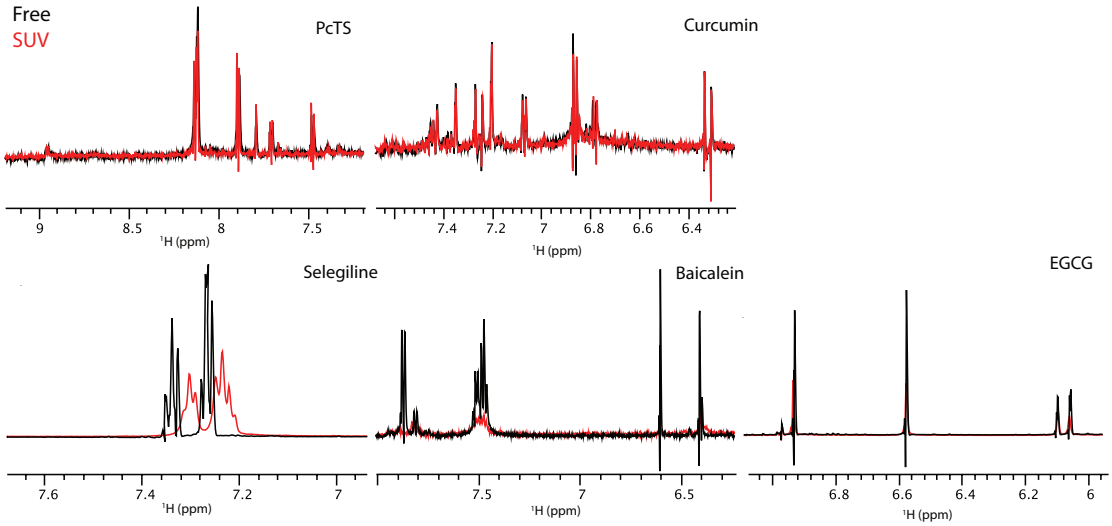

Supplementary Figure 2 | Selected region of the ^{1}H NMR spectra of the small molecules PcTS, curcumin, selegiline, baicalein and EGCG in the absence (black) and presence (red) of SUVs. Upon addition of vesicles, only the resonances of PcTS and curcumin remained unperturbed. Selegiline, baicalein and EGCG interact with vesicles and therefore show changes in NMR signal position and intensity. The final DMSO concentration was 1% of the total volume in 50 mM HEPES buffer, 100 mM NaCl, pH 7.4. NMR spectra were recorded at 288 K. Lipid and compound concentrations were 12.5 mM and 1.5 mM, respectively.

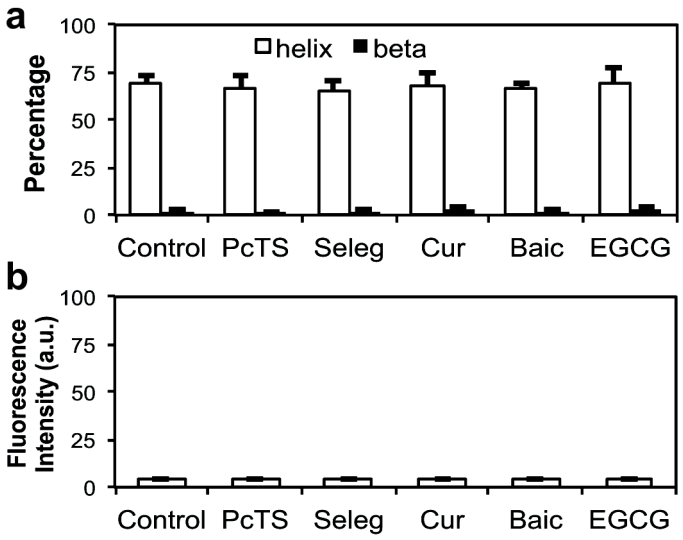

Supplementary Figure 3 | Conformational properties of αSyn prior to aggregation. (**a**) Secondary structure content of 100 μM fresh αSyn bound to 12.5 mM SUVs. Note that addition of a 15-fold excess of any of the compounds did not affect the binding of αSyn to SUVs and its vesicle-induced folding into a α-helical conformation. (**b**) ThT fluorescence signal before aggregation. Average values of at least 3 different samples.

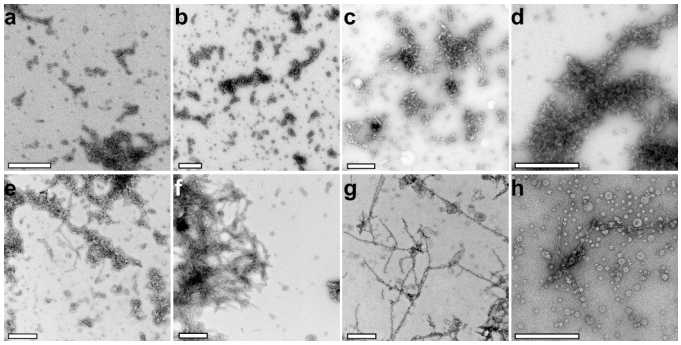

Supplementary Figure 4 | Electron micrographs of SUV-bound αSyn before (a-d) and after incubation for 10 days in aggregation-prone conditions (e-h) in the presence of selegiline (a,e), curcumin (b,f), baicalein (c,g) and EGCG (d,h). White bars represent 500 nm.

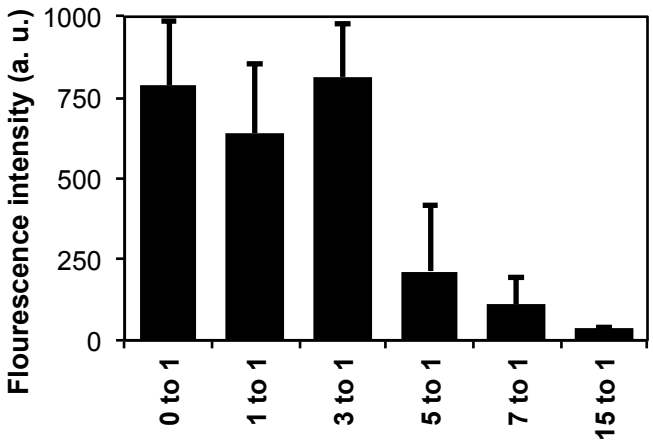

Supplementary Figure 5 | Influence of the concentration of PcTS on the aggregation of membrane-bound αSyn. Shown is the ThT fluorescence intensity after 10 days of incubation in aggregation prone conditions (37 °C with stirring). The concentration of αSyn was 100 μM, that of SUVs ~12.5 mM. The molar ratio of PcTS to protein ranged from 0:1 (no PcTS) to 15:1 (1.5 mM PcTS). Average values of at least 3 different samples.

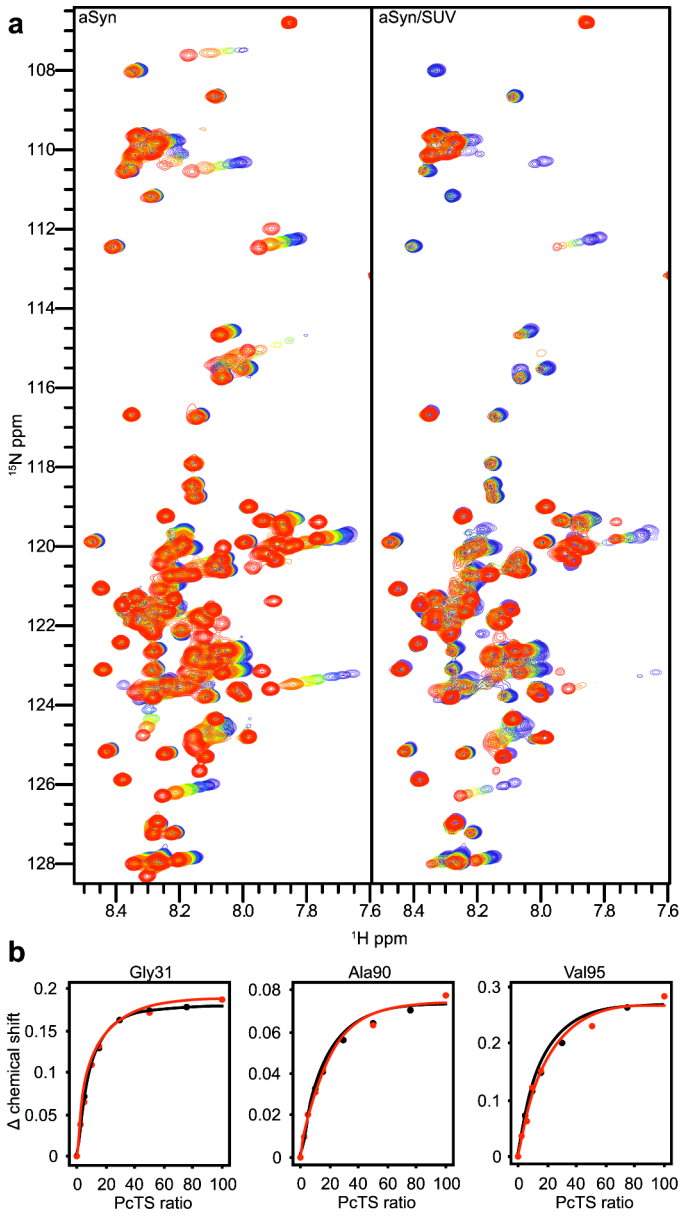

Supplementary Figure 6 | The presence of SUVs does not affect the affinity of PcTS to αSyn. (**a**) ^{15}N-^{1}H HSQC spectra of free (left panel) and SUV-bound (right panel) αSyn at increasing concentrations of PcTS (from red to blue). (**b**) Chemical shift changes as a function of PcTS concentration for selected residues in the presence (red line) and absence (black line) of SUVs.

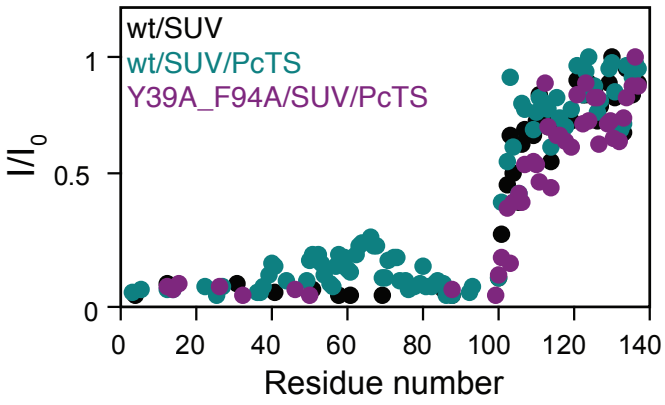

Supplementary Figure 7 | Residue-specific NMR signal intensity ratios obtained from ^{15}N-^{1}H HSQC spectra of 30 µM of αSyn recorded in the absence (I_0) and presence of 12.5 mM SUVs (I) (~417:1 lipid to protein molar ratio). Signal intensity ratios for *wt* αSyn in the absence (black) and in the presence (green) of PcTS are shown. Data for the Y39A/F94A variant of αSyn in the presence of PcTS are shown in purple. The concentration of PcTS was 0.45 mM (15:1 compound to protein molar ratio). Note that when residues are no longer in contact with liposomes, they become "visible" to solution NMR. Thus, even at higher lipid-to-protein ratios PcTS releases the NAC region of *wt* αSyn from the vesicle surface, but not that of the Y39A/F94A variant.

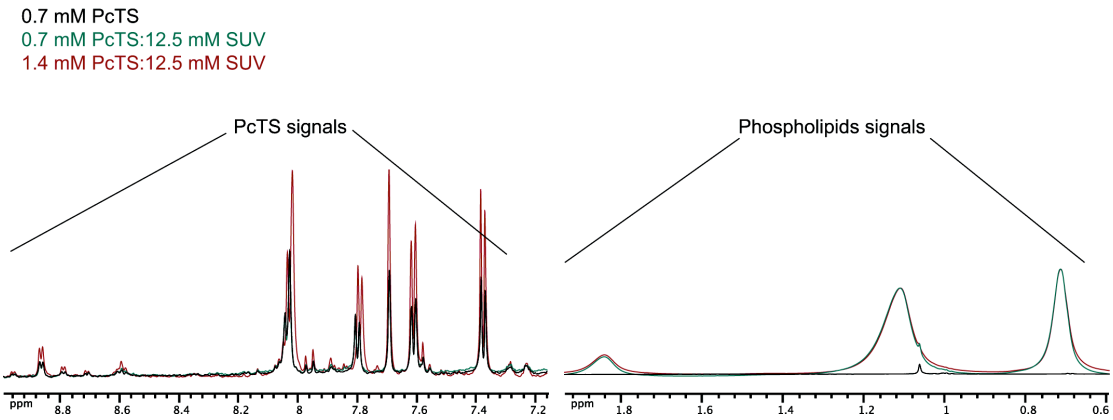

Supplementary Figure 8 | Proton NMR spectra show that PcTS does not interact with SUVs (left panel). Also, increasing amounts of PcTS do not fall out of solution by means of stacking within the concentrations used in the experiments.